

UCSF

UC San Francisco Previously Published Works

Title

Multiple breast cancer risk variants are associated with differential transcript isoform expression in tumors.

Permalink

<https://escholarship.org/uc/item/4wc9281k>

Journal

Human molecular genetics, 24(25)

ISSN

0964-6906

Authors

Caswell, Jennifer L
Camarda, Roman
Zhou, Alicia Y
et al.

Publication Date

2015-12-01

DOI

10.1093/hmg/ddv432

Peer reviewed

ASSOCIATION STUDIES ARTICLE

Multiple breast cancer risk variants are associated with differential transcript isoform expression in tumors

Jennifer L. Caswell^{1,2,3,5,*}, Roman Camarda^{1,3,4}, Alicia Y. Zhou^{1,3,4}, Scott Huntsman^{1,2,3}, Donglei Hu^{1,2,3}, Steven E. Brenner⁶, Noah Zaitlen^{1,2}, Andrei Goga^{1,3,4} and Elad Ziv^{1,2,3}

¹Department of Medicine, ²Institute for Human Genetics, ³Helen Diller Family Comprehensive Cancer Center and, ⁴Department of Cell and Tissue Biology, University of California, San Francisco, CA, USA, ⁵Department of Medicine, Division of Medical Oncology, Stanford University, Stanford, CA, USA and ⁶Department of Plant and Microbial Biology, University of California, Berkeley, CA, USA

*To whom correspondence should be addressed at: 875 Blake Wilbur Drive, Stanford, CA, 94305, USA. Tel: +1 3013326541; Fax: +1 4155144982; Email: caswell@stanford.edu

Abstract

Genome-wide association studies have identified over 70 single-nucleotide polymorphisms (SNPs) associated with breast cancer. A subset of these SNPs are associated with quantitative expression of nearby genes, but the functional effects of the majority remain unknown. We hypothesized that some risk SNPs may regulate alternative splicing. Using RNA-sequencing data from breast tumors and germline genotypes from The Cancer Genome Atlas, we tested the association between each risk SNP genotype and exon-, exon–exon junction- or transcript-specific expression of nearby genes. Six SNPs were associated with differential transcript expression of seven nearby genes at FDR < 0.05 (BABAM1, DCLRE1B/PHTF1, PEX14, RAD51L1, SRGAP2D and STXBP4). We next developed a Bayesian approach to evaluate, for each SNP, the overlap between the signal of association with breast cancer and the signal of association with alternative splicing. At one locus (SRGAP2D), this method eliminated the possibility that the breast cancer risk and the alternate splicing event were due to the same causal SNP. Lastly, at two loci, we identified the likely causal SNP for the alternative splicing event, and at one, functionally validated the effect of that SNP on alternative splicing using a minigene reporter assay. Our results suggest that the regulation of differential transcript isoform expression is the functional mechanism of some breast cancer risk SNPs and that we can use these associations to identify causal SNPs, target genes and the specific transcripts that may mediate breast cancer risk.

Introduction

Genome-wide association studies (GWASs) have identified thousands of disease risk-associated single-nucleotide polymorphisms (raSNPs), including, to date, 75 that are associated with breast cancer risk (1). The vast majority of raSNPs are located in noncoding regions of the genome; therefore, they, or SNPs in linkage disequilibrium (LD) with them, are likely to influence risk by

affecting the regulation of nearby genes or noncoding RNAs (2,3). To determine their function, investigators have tested their association with expression levels of nearby genes (expression quantitative trait loci, or eQTLs) in *cis* (4–7) or in *trans* (4) and assessed whether SNPs in LD with the index raSNP demonstrate evidence for transcription factor binding or histone methylation (6,8). These methods have uncovered eight eQTL associations (4,7), three associations with the targets of a nearby transcription

Received: May 6, 2015. Revised: September 10, 2015. Accepted: October 9, 2015

© The Author 2015. Published by Oxford University Press.

This is an Open Access article distributed under the terms of the Creative Commons Attribution License (<http://creativecommons.org/licenses/by/4.0/>), which permits unrestricted reuse, distribution, and reproduction in any medium, provided the original work is properly cited.

factor (4) and an enrichment of FOXA1 and ESR1 enhancer-binding sites within the rsSNP loci (8).

Another, yet unexplored, mechanism by which rsSNPs may affect regulation of nearby genes is through post-transcriptional regulation, such as alternative splicing. Previous work has used genome and transcriptome data from lymphoblastoid cell lines to systematically search for germline variants associated with the expression level of a specific transcript isoform of a gene (9–11). These genome-wide analyses have identified hundreds of splicing quantitative trait loci (splicing QTLs), typically exonic or intronic variants that affect exon skipping, alternative splice site inclusion, or the gene's 5' or 3' end sequence (9–11). GWAS variants are modestly enriched for splicing QTLs as well as for eQTLs (9), suggesting that some rsSNPs may affect risk by affecting differential transcript expression.

Modification of alternative splicing is known to be important in cancer development (12) and the epithelial-mesenchymal transition (13), and recent work has shown that somatic mutations affecting splicing can act as driver mutations in tumors (14). However, no systematic analysis has examined germline variants affecting cancer risk to identify, which may affect alternative splicing. In this paper, we develop methods to query whether a specific rsSNP functions as a splicing QTL of a nearby gene. Using publicly available data from The Cancer Genome Atlas (TCGA) (15), we perform a focused analysis of breast cancer rsSNPs, discovering five risk loci that may mediate risk by affecting differential transcript isoform expression.

Results

Splicing QTL analysis of breast cancer rsSNPs

We used the RNA-sequencing (RNA-seq) data and matched germline genotypes for 358 estrogen receptor (ER)-positive breast tumors and 109 ER-negative breast tumors from TCGA. For each of the breast cancer rsSNPs, we searched for differential transcript isoform expression of nearby genes (Supplementary Material, Table S1), adjusting for overall gene expression, global expression variability (16,17) and genetic ancestry. We used three complementary approaches, testing the association between rsSNPs and (1) rank-normalized reads per kilobase per million mapped reads (RPKM) mapping to each exon, (2) rank-normalized reads per million mapped reads (RPM) mapping to each exon–exon junction and (3) rank-normalized expression estimates of reconstructed transcripts of each annotated isoform, as generated by the RSEM algorithm using UCSC transcripts (chosen as its output is available through TCGA) (3) (Supplementary Material, Tables S2–S4). We identified 13 associations with 10 rsSNPs using these methods at FDR < 0.05, including 9 exon associations, 8 junction associations and 6 whole-transcript associations; several splicing QTLs were identified by more than one approach (Fig. 1). Q–Q plots showed deviation from normality at the extremes of the P-value distributions (Supplementary Material, Fig. S1). When the analysis was repeated in the smaller set of ER-negative tumors, we identified four associations with four rsSNPs, including two exon associations, two junction associations and two transcript associations (Supplementary Material, Table S5), all of which were also identified in the ER-positive tumors.

For the exon-specific test, we also tested for differences in raw counts mapping to each exon, using the negative binomial distribution as implemented by the DEXSeq R Bioconductor software package V1.8.0 (18). Of the nine SNP–gene exon associations identified using rank-normalized RPKM values, seven were significant

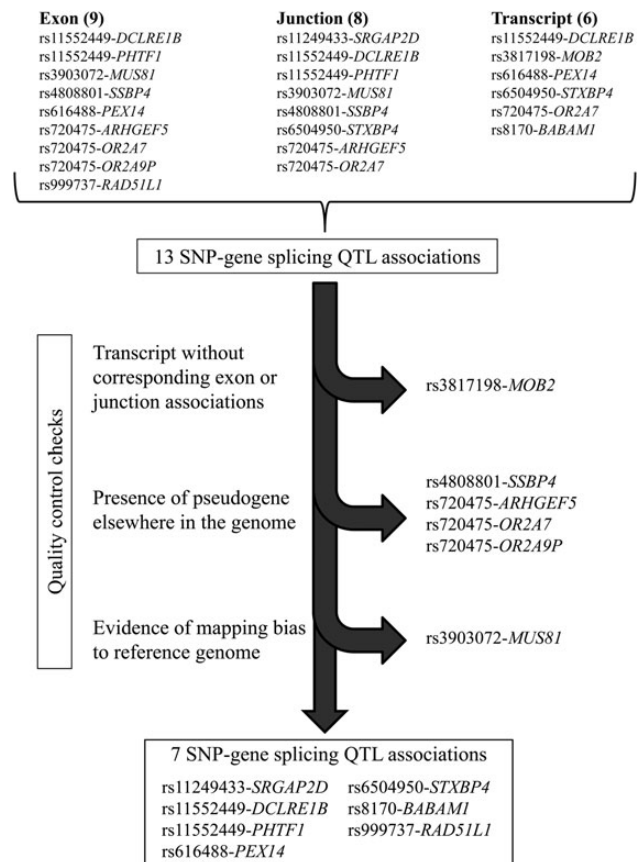


Figure 1. Flowchart for determining splicing QTL associations. We identified 13 SNP–gene associations through exon, junction and whole-transcript association tests with risk-associated SNPs; several associations were identified by multiple methods. After excluding SNP–gene associations that could not be corroborated with other tests, that could be related to the presence of pseudogenes or paralogs or that could have derived from mapping bias to the reference genome, seven SNP–gene associations remained.

at FDR < 0.05 when using DEXSeq, although the methods identified differing numbers of exons as significant (Supplementary Material, Table S6). One additional exon association (DCLRE1B) identified with rank-normalized RPKM values was captured because our test adjusted for overall gene expression with the exon of interest excluded, rather than because of a difference between rank-normalized RPKM values/linear regression versus raw counts/the negative binomial distribution. Given the similarity of the results, we used only normalization and linear regression for the remainder of the analyses.

We next excluded associations that could have resulted from one of three possible sources of error (Fig. 1). Associations identified through whole-transcript reconstruction require a high level of scrutiny because of inherent inaccuracies in transcript assembly, underscored by inconsistency in results from different methods (19). We therefore required associations identified through whole-transcript reconstruction to be supported by significant exon- or junction-specific associations, excluding one association (rs3817198-MOB2) that was not consistent with any exon- or junction-specific event at even a nominal level of significance. In contrast, the rs8170-BABAM1 association, also identified through whole-transcript reconstruction, was supported by increased expression of one exon 1–2 junction ($P = 1.9 \times 10^{-4}$) and decreased expression of another that used an alternate 3' acceptor site ($P = 0.024$).

We excluded four associations (two raSNPs) because the gene of interest had a paralog or pseudogene in another part of the genome. If a read can map to two different sections of the genome, the mapping algorithm's inaccuracy in placing it correctly can generate bias exacerbated by genetic variation (20). Rs720475 was identified as a splicing QTL for three genes: ARHGEF5, OR2A7 and OR2A9P. ARGHEF5 and OR2A7 are near-identical homologs; in a recent annotation of the genome [Gencode V19 (21)], OR2A7 has been extended and labeled ARHGEF34P. Similarly, OR2A9P is included in this region and represented by two pseudogenes 40 kb apart. Thus, the associations between rs720475 and expression of these three genes at least in part reflected difficulties in mapping reads that could come from multiple genes. The associations between rs4808801 and SSBP4 exons 2–4 were also excluded because of the presence of a retrotransposed pseudogene of SSBP4 on chromosome 18.

Finally, we excluded one association because of evidence of mapping bias to the reference genome. Mapping algorithms successfully map RNA-seq reads containing the reference allele more frequently than reads containing the alternate allele (22); eQTL and splicing QTL analyses may be susceptible to this bias if the exons contain SNPs in LD with the index raSNP. Four of the splicing QTL loci (including SSBP4, already excluded because of the presence of a pseudogene) contained an SNP in LD with the index raSNP ($r^2 > 0.1$) within the associated exon or junction. For each of these loci, we recalculated the association excluding all reads that mapped across such SNPs (Supplementary Material, Table S7). The associations between rs6504950 and STXBP4 and between rs11552449 and DCLRE1B remained significant. However, the associations between rs3903072 and MUS81 were not significant when excluding the reads that mapped to a pair of SNPs, rs659857 and rs545500. These SNPs are located two base pairs apart in MUS81 exon 6 and are in perfect LD with each other, an unusual situation that increases the potential for mapping bias.

After excluding the six problematic associations, six raSNPs were associated with exon, junction or whole-transcript expression of seven genes (Table 1). Four of the six loci replicated at $P < 0.05$ in the smaller set of 109 ER-negative tumors from TCGA (Table 1), three at FDR < 0.05 . We identified one SNP associated with exon skipping (rs11552449-DCLRE1B), two SNPs associated with alternative splice site usage (rs6504950-STXBP4 and rs8170-BABAM1) (Figs 2 and 3), three SNPs associated with more complex exon usage patterns (rs11552449-PHTF1, rs616488-PEX14 and rs999737-RAD51L1) and one SNP associated only with an exon–exon junction, which could represent an unannotated alternative splice site or other unannotated pattern of exon usage (rs11249433-SRGAP2D).

Relationship between breast cancer risk association and splicing QTL association

Because eQTLs and splicing QTLs are common throughout the genome (9,10,26), it is plausible that a raSNP could be associated with nearby gene or transcript expression but that this association would not be connected to breast cancer. To assess the possibility that the causal SNPs for the splicing QTL and the breast cancer association were different, we calculated the posterior probabilities of each of the SNPs at the locus as the causal SNP for each of the two traits. For the trait of breast cancer risk, we used association statistics from the GAME-ON website (<http://gameon.dfci.harvard.edu>). We then identified the most parsimonious list of SNPs that produced a cumulative posterior probability of >0.95 for the breast cancer association (Table 2). We then compared the cumulative

posterior probability of the splicing QTL associations for the same set of SNPs. We also repeated the inverse analysis, identifying the most parsimonious list of SNPs that produced a cumulative posterior probability of ≥ 0.95 of the splicing QTL association and found the cumulative posterior probability of the GWAS association from the GAME-ON data (Supplementary Material, Table S9).

For some of the loci, such as STXBP4, SRGAP2D and RAD51L1, the breast cancer association is highly significant and thus the number of likely SNPs is relatively small. For the STXBP4 locus, we were able to narrow the list of SNPs at the locus from 908 to 40 and noted a very high probability (0.99) that the splicing QTL causal variant was also captured in this set. Conversely, starting with the splicing QTL, we narrowed the SNPs down to 23 and found a posterior probability of 0.55 that the GWAS causal variant was also captured in this set. For the SRGAP2D locus, starting with the GWAS data, we narrowed the list of likely SNPs from 37 to 3, and the posterior probability that the splicing QTL was determined by these three SNPs was 4×10^{-7} . Conversely, starting with the splicing QTL data, we only narrowed down the list of SNPs from 37 to 23 but still found that the posterior probability of the causal SNP for GWAS was ~ 0.01 . Thus, we excluded the possibility that the splicing QTL and breast cancer association are caused by the same variant at this locus. For RAD51L1, we narrowed the list of likely SNPs at the locus from 1152 to 11, and the posterior probability of the 11 SNPs for the splicing QTL was 3×10^{-9} . Similarly, starting with the splicing QTL, we narrowed the signal to five SNPs which had a posterior probability of the GWAS SNP of $\sim 1 \times 10^{-9}$. Therefore, we also excluded the possibility that the case–control and exon 15 splicing QTL effect are caused by the same variant. Interestingly, when examining the association of each individual exon of the gene with the raSNP (Supplementary Material, Fig. S2), we noted that the raSNP for RAD51L1 was associated with several different exons, though only exon 15 at FDR < 0.05 . In the reconstructed transcript test, the raSNP for RAD51L1 was also associated ($P = 7.3 \times 10^{-4}$), though not at FDR < 0.05 , with transcript uc001xkf, which includes exon 14 rather than exon 15. This transcript had greater overlap of the posterior probability with the breast cancer association. This analysis suggests that it may be possible to use this Bayesian approach to disentangle not only whether the causal SNP for a splicing QTL and for breast cancer risk are the same but more precisely which transcript is in fact associated with breast cancer risk.

At other loci, the breast cancer association statistics were less significant and consequently our ability to narrow down the set of plausible SNPs, and to dissect the splicing QTL association from the breast cancer association, was more limited. We note that at the PEX14 locus, the overlap with the posterior probability for breast cancer was higher for transcript uc001arm than for exon 7, hinting at the possibility that it is this entire transcript rather than simply exon 7 that is implicated in breast cancer risk. At the DCLRE1B/PHTF1 locus, we were unable to definitively rule out one of those genes when we examined the overlap with the posterior probability of breast cancer. Similarly, the posterior probability at the BABAM1 locus included a large number of SNPs that we could not narrow effectively based on the breast cancer association.

Leveraging splicing QTLs to identify causal SNPs

Once a raSNP is identified through GWAS, a major challenge is discerning which of the many possible SNPs in LD with the initially identified SNP might be causal (2). The link between the raSNP and the expression of a particular splice junction or exon

Table 1. Splicing QTLs identified in ER-positive tumors at FDR < 0.05, after exclusions

SNP rsID	Gene Component	β (ER+)	P-value (ER+)	FDR (ER+)	P-value (ER-)	Predicted splicing pattern associated with breast cancer risk
rs6504950	STXBP4					Longer exon 6 (6 bp 5'): \uparrow use of 3' acceptor site at chr17:53 076 993 and \downarrow use of chr17:53 076 987
	Exon 5:6 junction 1	-0.73	5.5E - 24	8.3E - 20	1.9E - 11	
	Exon 5:6 junction 2	0.59	1.9E - 23	1.4E - 19	1.6E - 07	
	Transcript uc010dcc	-0.42	3.5E - 11	4.4E - 08		
rs11552449 ^a	DCLRE1B					\uparrow exon 2 inclusion
	Transcript uc001eei	-0.64	8.6E - 14	1.6E - 10	2.4E - 06	
	Transcript uc001eeg	0.26	2.2E - 10	2.3E - 07	4.4E - 05	
	Exon 1:3 junction	-0.48	7.0E - 08	4.5E - 05	4.5E - 03	
	Exon 2	0.24	2.7E - 08	2.1E - 05	6.1E - 06	
rs8170	BABAM1					Longer exon 2 (38 bp 5'): \uparrow use of 3' acceptor site at chr19:17 379 565
	Transcript uc002nfv	0.47	3.0E - 08	2.1E - 05	8.2E - 06	
	Transcript uc002nfu	-0.29	2.7E - 07	1.7E - 04	0.038	
rs11249433	SRGAP2D					^b
	Exon 2:3 junction	-0.39	1.3E - 08	1.2E - 05		
rs11552449 ^a	PHTF1					\uparrow inclusion of exons 1 and 2
	Exon 1:2 junction	0.47	3.0E - 08	2.1E - 05		
	Exon 2	0.28	1.9E - 06	9.0E - 04		
rs616488	PEX14					\downarrow transcript uc001arm (exons 1, 2, 6, 7)
	Exon 7	-0.39	3.8E - 07	2.2E - 04	0.021	
	Transcript uc001arm	-0.39	5.1E - 07	2.8E - 04		
rs999737	RAD51L1					\downarrow transcript uc001xkf (exons 1-11, exon 14)
	Exon 15	-0.33	2.3E - 05	9.1E - 03		

β is for the effect of the breast cancer risk allele on the gene component.

bp, base pairs.

Transcripts are named according to UCSC ID. Genomic positions are for hg19 build.

P-values for ER-negative tumors displayed when is <0.05.

^aSNP is associated with transcript expression of two different genes.

^bSplicing QTL association not predicted to be linked to breast cancer given pattern of association at locus.

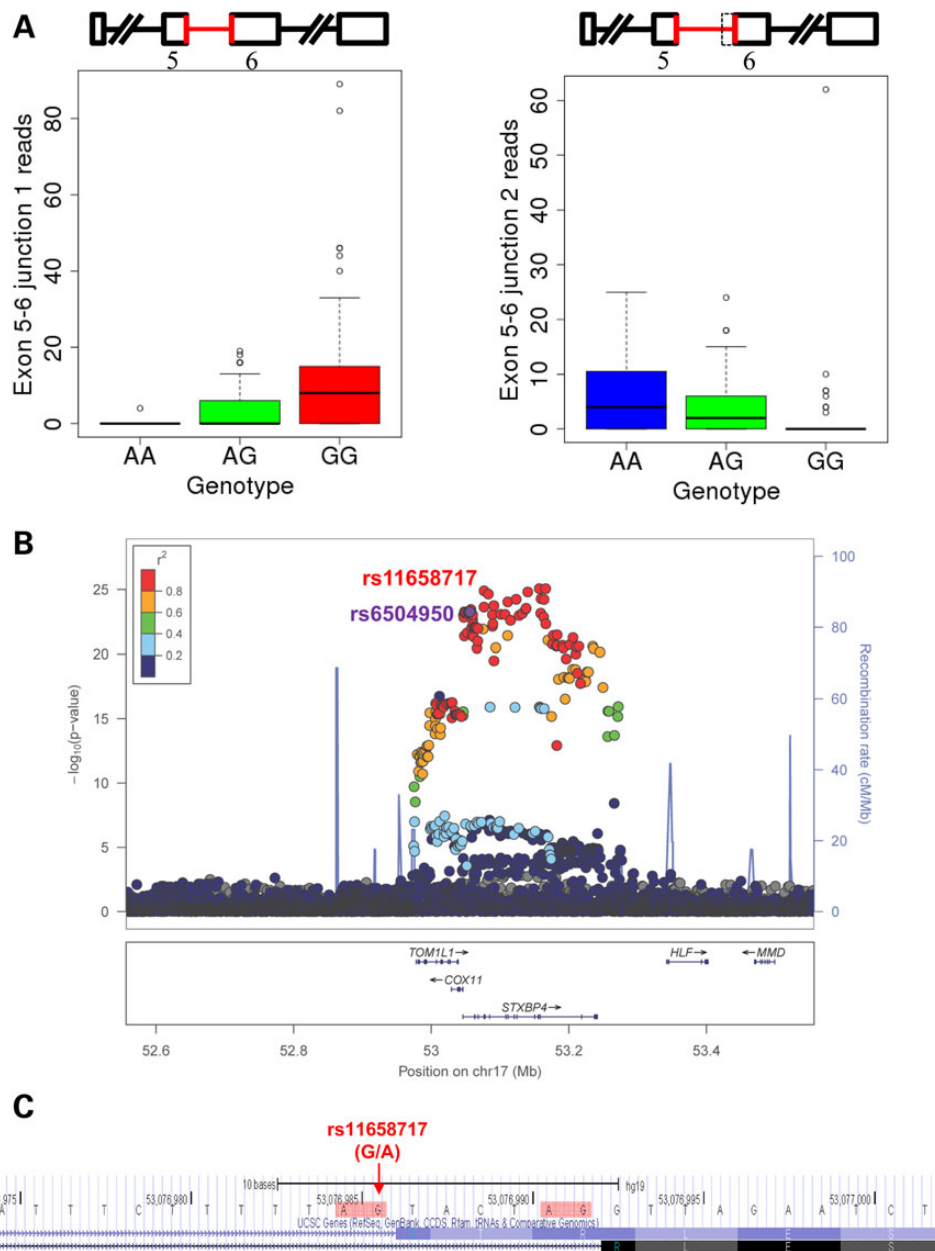


Figure 2. Alternative splice site usage in STXBP4 exon 6 based on rs6504950 genotype. (A) With the rs6504950 risk allele, virtually all STXBP4 exon 5–6 junction reads map to one junction, whereas with the non-risk allele, virtually all map to the other. (B) LocusZoom plot (23) displaying $-\log_{10}$ P-values for the association of each SNP within the window with STXBP4 exon 5–6 junction 1 by position. (C) The locus of rs11658717, the presumed causal SNP. The two alternative 3' splice sites are highlighted in red. The minor allele of rs11658717 (G) is in high LD with the risk allele of rs6504950 (A). Screenshot from <http://genome.ucsc.edu> (24).

can shed new light on the identity of the causal SNP, as in some cases only one or a few SNPs in LD with the original raSNP may be likely able to affect alternative splicing by virtue of their location within the gene. Examining all known variants from 1000 Genomes in each splicing QTL region, we were able to narrow the list of possible functional SNPs for three of the six splicing QTLs predicted to be associated with breast cancer (Supplementary Material, Table S8).

In two cases, the association of the raSNP with alternative splice site usage allowed us to identify the specific likely causal SNP. At the STXBP4 locus, rs6504950 was associated with increased usage of one 3' acceptor site of intron 5 of STXBP4 and decreased usage of another that was six bases distant

(Fig. 2). Of 177 SNPs in LD with rs6504950 at $r^2 > 0.6$, only one (rs11658717) was in intron 5, where it altered an AG 3' acceptor site to AA; as expected, with the G allele, virtually all transcripts appeared to use the first of the two possible 3' acceptor sites, whereas with the A allele, virtually all transcripts appeared to use the second. Interestingly, not only was rs11658717 more associated with the exon 5–6 junctions than was rs6504950, it was also modestly more associated with breast cancer risk (Supplementary Material, Table S8) (27).

Similarly, rs8170 was associated with increased usage of one 3' acceptor site in intron 1 of BABAM1 and decreased usage of another. Of 34 SNPs in LD with rs8170 at $r^2 > 0.6$, only one was located in the first intron (Fig. 3). This SNP, rs10424178, lies within

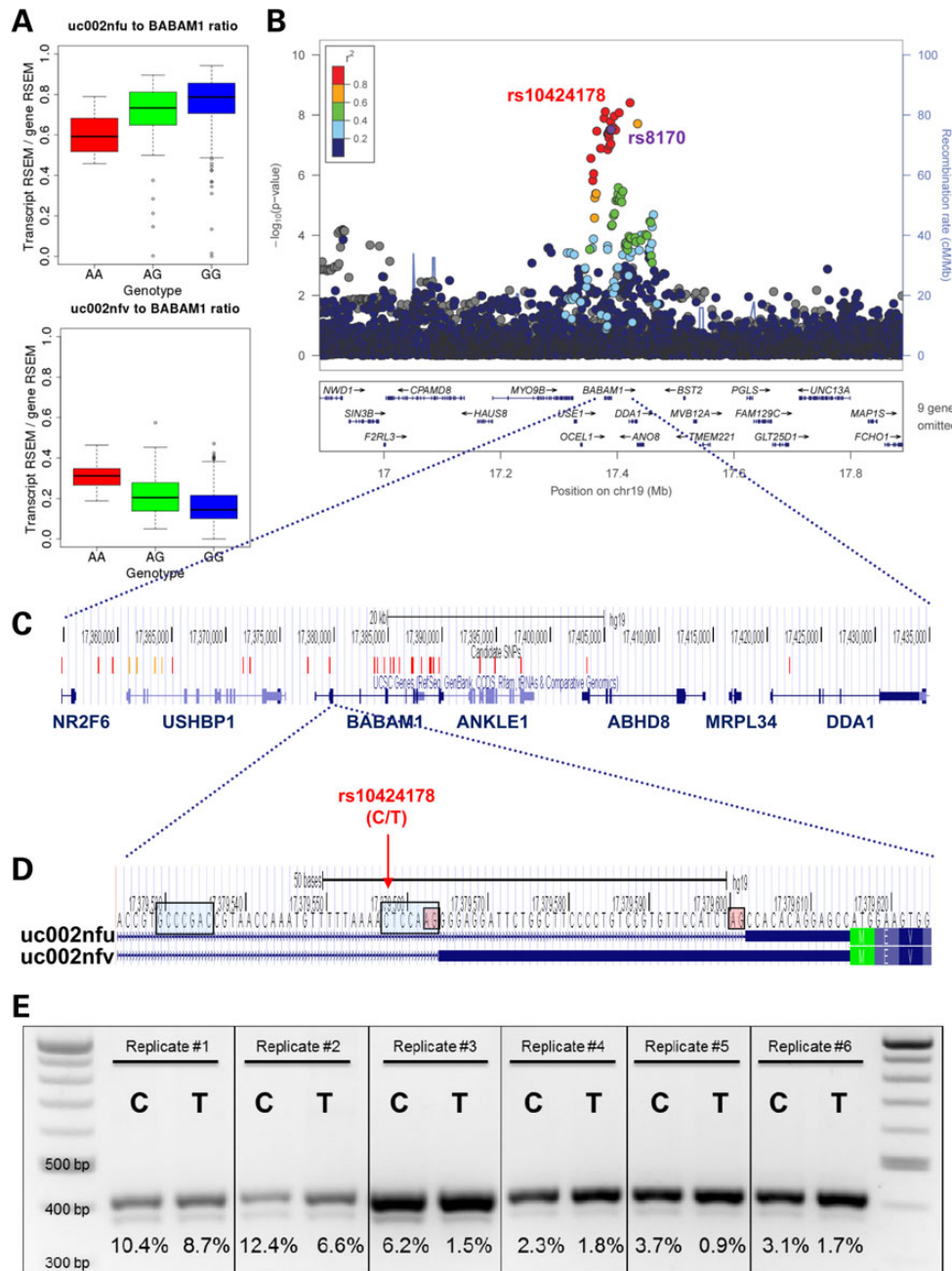


Figure 3. Alternative splice site usage in BABAM1 exon 2 based on rs10424178 genotype. (A) Relative expression of RSEM reconstructed BABAM1 transcript uc002nfu decreases and uc002nfv increases with rs10424178 risk genotype. (B) LocusZoom plot (23) displaying $-\log_{10}$ P-values for the association of each SNP within the window with BABAM1 uc002nfv transcript expression by position. (C) Locations of all candidate SNPs, defined as SNPs with $r^2 > 0.6$ with rs10424178, or LD unknown but splicing QTL association P-value of $< 1 \times 10^{-6}$. SNPs are colored red if $r^2 > 0.8$ and orange if $r^2 > 0.6$. Screenshot from <http://genome.ucsc.edu> (24). (D) The locus of rs10424178, the presumed causal SNP. The two alternative 3' splice sites are highlighted in red, and the two alternative branch points as identified by Human Splicing Finder (25) are highlighted in blue. The minor allele of rs10424178 (T) is in high LD with the risk allele of rs8170. Screenshot from <http://genome.ucsc.edu> (24). (E) Results of a six replicates of a minigene reporter assay, transfecting the major allele (C) or minor allele (T) of rs10424178. In each well, the lower band represents the shorter BABAM1 exon 2, as included in transcript uc002nfu, and the upper band represents the longer BABAM1 exon 2, as included in transcript uc002nfv; the identities of the bands were confirmed by sequencing. The percentages shown below each well are the intensity of the lower band divided by the sum of the intensities of the lower band and the upper band. In all six replicates, the percentage of the total bands represented by the shorter BABAM1 exon 2 is higher for the major allele than that for the minor (risk) allele.

the predicted branch point sequence (25) for the second 3' acceptor site and is 5 bases 3' of the first 3' acceptor site. Like rs11658717, rs10424178 was more strongly associated than the index rsSNP with the transcript expression (Supplementary Material, Table S8); data for its association with breast cancer risk were not available.

To test whether the alteration of the branch point sequence by rs10424178 caused the predicted splicing difference *in vitro*, we cloned the BABAM1 exon 2 and flanking intronic sequence into two minigene plasmid vectors, each containing an alternate allele of rs10424178, transfected each vector into cells and

Table 2. Overlap of the posterior probabilities of the splicing QTL and case-control association statistics based on cumulative probability of case-control association of >0.95

	Target event	Best P-value for breast cancer from GAME-ON	Total number of SNPs	Number of SNPs to reach 0.95 probability case-control	Splicing QTL cumulative probability
Locus 1	STXBP4	5.2×10^{-5}	908	54	0.99
Locus 2	DCLRE1B	2.0×10^{-3}	705	337	0.99
Locus 2	PHTF1		705	337	>0.99
Locus 3	BABAM1*	5.1×10^{-3}	588	452	>0.99
Locus 4	SRGAP2D	4.0×10^{-8}	37	3	4.3×10^{-9}
Locus 5	PEX14-exon7	8.3×10^{-4}	537	90	0.60
Locus 5	PEX14-transcript uc001afk		537	90	0.97
Locus 6	RAD51L1-exon15	6.9×10^{-11}	1151	11	9.2×10^{-8}
Locus 6	RAD51L1-transcript uc001xkf		1151	11	0.29

*P-value for BABAM1 was obtained from the ER-negative analysis from GAME-ON, because this locus was identified by a GWAS for ER-negative breast cancer.

measured the gel band intensity of the two BABAM1 transcript components (28). In all six replicates, the minor allele was associated with relatively lower usage of the second of the two 3' acceptor sites (Fig. 3e): on average, 3.5% of transcripts had the shorter exon 2 with the minor allele compared with 6.4% with the major allele (paired t-test, $P = 0.02$). This pattern corresponded to what was seen in the TCGA RNA-seq data of the tumors, validating the functional effect of rs10424178 at the locus.

Discussion

The majority of disease raSNPs are in noncoding regions of the genome (1), and these noncoding raSNPs are presumed to influence regulation of nearby genes. Here, we show that six breast cancer raSNPs are associated with differential isoform expression of seven nearby genes in breast tumors. At five of these loci, the top splicing QTL SNPs are also in high LD with the top breast cancer associated SNPs. Our results suggest that regulation of alternative splicing is perhaps nearly as important as mechanism in affecting breast cancer susceptibility as regulation of overall gene expression: there are eight eQTLs that have been reported in breast tissue with these same breast cancer risk loci (4,7).

Current pipelines for discerning the functional effects of GWAS raSNPs focus on eQTL analyses and searching for associated potential causal variants within coding, transcriptional start site or enhancer regions using systematic annotation of the genome for these sites (2,4,6–8,29–31). The findings of this study suggest that splicing QTL analyses, as outlined here, should be included to help illuminate the function of raSNPs and that systematic annotation of genomic regions crucial for splicing will be important in interpreting the results from GWAS. Careful examination of putative associations is essential to determine that an apparent splicing QTL effect is not an artifact of mapping error or bias in RNA-sequencing data. Minigene splicing reporter assays can confirm the splicing effects of the predicted causal SNPs *in vitro*, much as luciferase reporter assays can confirm the effects of predicted causal SNPs in enhancer regions.

In addition to uncovering causal SNPs, splicing QTL associations can help clarify which candidate gene affects breast cancer risk. For example, rs8170 is in LD with SNPs, which lead to missense variants in ANKLE1 (6), but our analyses implicate BABAM1 as the causal gene at this locus. This result is consistent with the known interaction of BABAM1 with BRCA1, and with the

fact that rs8170 modifies the risk of BRCA1 mutation carriers (32). Furthermore, beyond identifying the candidate gene, the splicing QTL associations implicate a particular exon or domain of that gene as important in breast cancer risk. For example, not simply the BABAM1 gene but an extra 38 base pairs of its 5' untranslated region is associated with increased breast cancer risk. Similarly, two fewer amino acids in the sixth exon of the STXBP4 gene are associated with increased breast cancer risk. Additional experiments examining the effects of the particular transcripts we identified to be associated with breast cancer risk should enhance our understanding of breast cancer susceptibility.

We also developed an approach that compares the posterior probability of the causal SNPs for the expression phenotype with the breast cancer phenotype. Previous studies have also examined the likelihood that the causal SNP for an expression phenotype is the same as that for a disease trait (33). Our method is similar to the approach of Giambartolomei *et al.* (34) that calculates the posterior probability of the same SNP being causal for the gene expression and disease risk locus. However, our method is different in that it assumes that there is both a real gene expression association and disease association at the locus and that the only two possibilities are that they are due to the same causative SNP versus different causative SNPs. In contrast, Giambartolomei *et al.* consider a wider range of possibilities including ones that do not have an expression association or disease association at the locus. As we started with loci that had been validated as GWAS hits for breast cancer and with a stringent FDR for association for gene expression, the priors of no association for either of these were not valid. Our approach was limited by the P-values at some of the loci that were available from GAME-ON. In particular, for the loci defined by rs11552449 and rs8170, the GWAS signals in the GAME-ON dataset are in the range of P-values of 0.01 to 0.001, which is likely insufficient to draw conclusions about the co-localization of the GWAS signal. As larger datasets with more comprehensive SNP coverage become available, the other loci may produce clearer results.

Our study has several limitations. First, we used breast tumor tissue, rather than normal tissue, to identify putative splicing QTLs among the breast cancer raSNPs. A challenge in eQTL analyses has been using tumor tissue, of which there is much more available expression data, to identify these effects in the face of the acquired somatic genetic and epigenetic changes that occur within tumors. Methods have been developed to adjust eQTL analyses performed in tumor tissues for certain somatic alterations, including copy number and methylation status (4). These

factors are well understood to affect overall gene expression, but their effects on alternative splicing patterns are, to date, less well understood and more difficult to quantify. However, it is becoming clear that methylation of splice sites can lead to variation in alternative splicing (35) and that intragenic translocation events can affect exon inclusion or exclusion, for example in small cell lung cancer (36). It remains possible that these or other recurrent somatic changes, such as somatic mutations affecting splicing (14), could affect alternative splicing patterns in ways unmeasured in our analyses. While these somatic changes may blur the mechanism connecting a raSNP to its associated change in alternative splicing, the associations should remain valid: for example, the association between a raSNP and exon exclusion might in fact be dictated by its association with an intragenic translocation event, with methylation of a splice site or as, initially hypothesized, with the splicing event itself. Repeating splicing QTL analyses in normal tissues as they become available, for example with the development of the Genotype-Tissue Expression database (37), will be instructive. However, ultimately, functional validation of the impact of the genetic variant on the alternative splicing pattern in an *in vitro* setting, as we performed with the rs8170-BABAM1 association, is necessary to confirm the alternative splicing changes observed in any tissue.

A second limitation is that we limited our assembled transcript data to those produced by TCGA, namely using one transcript definition (UCSC) and one method of transcript assembly (RSEM), though different methods are known to produce different results (19). By requiring associations identified through whole-transcript reconstruction to be supported by the focused tests of exons and junctions, we eliminated some of the erroneous associations caused by transcript assembly. Nonetheless, we found transcript reconstruction valuable, as it hinted at situations where whole transcripts, rather than just exons or splice sites, were implicated in breast cancer risk (RAD51L1). Third, we have shown that mapping bias has the potential to generate false-positive results. While we removed all identified problematic associations, it remains possible that there are unknown variants in the exons and junctions generating unmeasured bias. Fourth, we note that the fact that a raSNP is associated with transcript expression does not mean its effect on breast cancer risk is mediated through that transcript. In fact, we were able to exclude this possibility at one locus (SRGAP2D). While we attempted to use information about association with breast cancer risk at the loci to determine which splicing QTLs were likely to be connected to breast cancer, functional studies are necessary to confirm the link between change in expression pattern and cancer risk.

In summary, we have identified seven novel associations between SNPs discovered by GWAS for breast cancer and alternatively spliced isoforms of genes in *cis*, five of which are consistent with mediating the association between raSNP and breast cancer risk. These splicing QTL associations help identify likely causal SNPs and candidate genes and also implicate specific alternatively spliced variants of those genes that mediate the effect on breast cancer susceptibility. Our results suggest that SNPs affecting alternative splicing may play an important role in breast cancer and possibly other complex genetic traits.

Methods

Germline genotypes and imputation

We downloaded the Affymetrix SNP6.0 germline genotypes from TCGA (<http://cancergenome.nih.gov>; date of download 17 December 2012). To obtain genotypes for the breast cancer raSNPs

that were not directly genotyped in TCGA, as well as other regional SNPs for fine-mapping, we phased using Shapeit V2 (38) and imputed to the 1000 Genomes phase 1 V3 reference panel (39) using IMPUTE2 (40). We used the imputed 'dosage' values (that is, the means of the distribution of imputed genotypes) in association analyses, which allows for uncertainty about the true genotype to be incorporated into the association test (41). All 75 breast cancer raSNPs were either directly genotyped in TCGA or had an INFO score of ≥ 0.5 .

Splicing QTL association analyses

All statistical analyses were performed with the R programming language V2.15.3. We divided ER-positive ($N = 358$) and ER-negative ($N = 109$) tumors based on ER-status in the TCGA clinical data. We performed all analyses on ER-positive and ER-negative tumors separately.

We downloaded the Level 3 TCGA RNA-seq data (<http://cancergenome.nih.gov>; date of download 30 December 2013) listing the RPKM values and raw reads (used for DEXSeq analysis) for each defined exon counting bin, number of reads mapping to each defined exon-exon junction and RSEM expression estimates for each annotated gene and transcript. We rank-normalized the RPKM values within each exon counting bin, replacing each RPKM value with its fractional rank (that is, its position in the ordered array of all values divided by the total number of values) and transforming that rank onto the standard normal distribution (42). For junction analysis, we adjusted the raw reads value for the number of total reads per sample to obtain RPM values and then rank-normalized these values according to the same method. For transcript analysis, we similarly rank-normalized the RSEM values for the reconstructed transcripts.

For each linear regression analysis (exon, junction and transcript), we adjusted for the overall expression of the gene, genetic ancestry using the first three principal components identified using EIGENSTRAT (43) on the genotypes of all TCGA samples and global expression variability using the first three factors identified using PEER analysis (16,17) on the \log_2 (RPKM + 0.25) values of exons from the entire TCGA RNA-seq dataset (on ER-positive and ER-negative tumors separately). For both principal component analysis and PEER factor analysis, the first identified principal component or factor explained the vast majority of the variance of the samples, and we chose to use the first three as covariates as there was a subsequent leveling off in proportion of variance explained (Supplementary Material, Fig. S3).

For exon analysis, we tested the association of each raSNP with each exon of each gene containing two or more exons within ± 500 kb:

$$\text{RPKM}_{\text{exoni}} = \beta_0 + \beta_1 g + \beta_2 \left[\left(\sum_{j=1}^n \text{RPKM}_{\text{exonj}} \right) - \text{RPKM}_{\text{exoni}} \right] + \beta_3 \text{PC1} + \beta_4 \text{PC2} + \beta_5 \text{PC3} + \beta_6 \text{K1} + \beta_7 \text{K2} + \beta_8 \text{K3},$$

where $\text{RPKM}_{\text{exoni}}$ is the rank-normalized RPKM for the tested exon, g is the genotype at the raSNP (the dosage value where imputed, ranging from 0 to 2), n is the number of exons in the gene, PC1 through PC3 are the first three principal components and K1 through K3 are the first three factors identified through PEER (16,17). In the exon analysis, when we adjusted for overall gene expression, we subtracted the RPKM of the tested exon so as not to diminish the power of the test in genes with very few exons, where the overall gene expression may be strongly correlated with the expression of the tested exon. For junction

analysis, we tested the association of each raSNP with each exon–exon junction within ± 500 kB:

$$\text{RPM}_{\text{junction}} = \beta_0 + \beta_1 g + \beta_2 \text{RSEM}_{\text{gene}} + \beta_3 \text{PC1} + \beta_4 \text{PC2} + \beta_5 \text{PC3} + \beta_6 K1 + \beta_7 K2 + \beta_8 K3.$$

For transcript analysis, we tested the association of each raSNP with each transcript of each gene with two or more annotated transcripts within ± 500 kB, excluding transcripts that had zero expression in $>25\%$ of samples:

$$\text{RSEM}_{\text{transcript}} = \beta_0 + \beta_1 g + \beta_2 \text{RSEM}_{\text{gene}} + \beta_3 \text{PC1} + \beta_4 \text{PC2} + \beta_5 \text{PC3} + \beta_6 K1 + \beta_7 K2 + \beta_8 K3.$$

We used the DEXSeq R Bioconductor software package V1.8.0 (18) to test for differential exon expression between genotypes using raw exon counts and the negative binomial distribution. For dispersion estimates in association tests, given the number of samples, we did not apply exon sharing with `fitDispersionFunction()`, instead using the dispersion parameter of each exon calculated independently. We used the first ten principal components from EIGENSTRAT as covariates. Supplementary Material, Figure S2 was obtained using the `plotDEXSeq()` function of the DEXSeq package.

Evaluation for mapping bias

To assess for evidence of mapping bias, we downloaded the Level 1 RNA-seq BAM files for the 358 ER-positive tumors with matched germline genotypes from TCGA (date of download 7 May 2014). We identified all SNPs from 1000 Genomes phase 1 V3 (39) or HapMap phase 2 (44) that were in LD with the index SNP with $r^2 > 0.1$ in the European (1000 Genomes) or CEU (HapMap) populations and lay within a site (exon or junction) found to be associated with risk genotype. For each relevant association, we counted all reads mapping to the site of interest excluding reads that mapped to those SNPs and recalculated the association with the raSNP genotype, adjusting for overall expression of the gene and genetic ancestry.

Splicing QTL fine-mapping

For the 358 ER-positive tumors, we obtained the genotypes of all SNPs from 1000 Genomes phase 1 V3 that were within ± 500 kB of each index raSNP that had been identified as a splicing QTL, that had minor allele frequency of >0.001 in TCGA samples and, if imputed as described previously, that had an INFO score of >0.5 . We then calculated the P-value for the association of each of these SNPs with the exon, junction or transcript expression that we had identified as being most significantly associated with the index raSNP. We used the LocusZoom software (23) to generate plots of the splicing QTL P-values against genomic position, colored by LD r^2 as calculated from the European population in 1000 Genomes. We used Human Splicing Finder V2.4.1 (25) to annotate alternative splice sites and branch point sequences. We searched for P-values for breast cancer risk association of SNPs in the GAME-ON meta-analysis of breast cancer risk case–control studies (27); if data for the SNP of interest were not available, we used the SNP with the highest r^2 with the index SNP in the European population in 1000 Genomes. Figures 2c and 3c and c were obtained using the UCSC Genome Browser (24).

Evaluating overlap of GWAS and splicing QTL signal

We first calculated the posterior probabilities that each SNP at the locus was the causal SNP for case–control association. We then repeated this process for the splicing QTL signal. For the case–control association, we downloaded all of the association statistics from the 1MB region around the index GWAS SNP from the GAME-ON website (<http://gameon.dfc.harvard.edu>). We merged the SNP list between the splicing QTL association analysis, which had been imputed to 1000 Genomes (39) and the case–control association, which had been imputed to Hapmap version II (44), and generated a list of overlap SNPs. To calculate the posterior probabilities for each SNP in the dataset being the causal SNP, we used a modification of the approach we have previously developed (45). We started with the observed vector Z of z scores from the case–control association test for each of the SNPs and the observed LD matrix Σ , which includes the elements r_{ij} for each pair of SNPs where r is the LD coefficient where i and j represent individual SNPs from the list of n SNPs at the locus.

For each SNP, i , we calculated another matrix M_i whose elements μ_j are equal to $z_i \times r_{ij}$, which are the expected z statistics assuming that SNP i is causal (46). We then calculated the likelihood, ℓ_i , of SNP i being the causal SNP conditional on the observed vector Z , the expected vector M and the observed matrix, Σ , using the inverse of the multivariate normal distribution: $\ell_i = \Phi^{-1}(Z, M, \Sigma)$. We repeated this process for each SNP, getting a new vector ℓ of elements ℓ_i . The posterior probability P_i of each SNP i is calculated as follows:

$$P_i = \frac{\ell_i}{\sum_{j=1}^n \ell_j},$$

where n is the number of elements in ℓ .

We repeated this analysis for the splicing QTL analysis. To derive Z scores for the SNPs from the splicing QTL analysis, we calculated the Z statistics based on an inverse normal transformation from P-values derived from the linear regression models and used the signs from the β coefficients from the model.

Finally, to determine the overlap between the two sets of signals, we ordered the posterior probabilities from the case–control analysis from highest to lowest. We then identified the minimal number of SNPs required to produce a cumulative posterior probability of >0.95 of having the causal variant. If the cumulative sum of the posterior probability of the GWAS was <0.05 when the cumulative sum of the posterior probability of the splicing QTL association was >0.95 , we concluded that the two associations were likely to be due to a different causal variant.

Minigene splicing reporter assay

We synthesized two sequences corresponding to BABAM1 exon 2, 50 base pairs of flanking 3' intronic sequence and 100 base pairs of flanking 5' intronic sequence, one with the major (C) and one with the minor (T) allele of rs10424178, with an upstream SalI and a downstream XbaI restriction enzyme site (purchased from IDT DNA). We subcloned these sequences into the RHCglo minigene splicing reporter construct (28) by SalI and XbaI restriction enzyme digest and ligation. Both SNP variation subclones were verified by sequencing.

We then plated HEK293T cells at 1×10^6 cells/60-mm culture dish in 4 ml growth medium (DMEM with 10% fetal bovine serum, 1% penicillin–streptomycin and 1% l-glutamine; GIBCO Life Technologies). Twenty-four hours after plating, we transfected

cultures with 1 µg of the minigene plasmid using Lipofectamine 2000 (Life Technologies). We extracted total RNA 24 h post-transfection by mirVana miRNA Isolation Kit (Life Technologies). We performed RT-PCR on 1 µg of total extracted RNA to generate cDNA using the iScript cDNA Synthesis Kit (Bio-Rad). We performed PCR on 200 ng of the generated cDNA using the MyTaq Red Mix (Bioline). The upstream primer was RSV5U, and the downstream primer was TNIE4 as previously described (28). PCR products were subject to electrophoresis on a 3% agarose gel and imaged and quantified by ChemiDoc XRS+ (Bio-Rad).

Supplementary material

Supplementary Material is available at HMG online.

Acknowledgements

The authors thank Nasim Ahmadiyeh, Laura Fejerman, Matthew Freedman and Christopher Haiman for their conceptual input, and Tom Cooper for supplying the RHCglo minigene splicing reporter. The results published here are in part based upon data generated by the TCGA Research Network: <http://cancergenome.nih.gov>. DRIVE, funded by NCI Grant number U19 CA148065, assembled the data and generated the website used for breast cancer GWAS data: <http://gameon.dfci.harvard.edu>. Many computations were performed using the UCSF Biostatistics High Performance Computing System and the Institute for Human Genetics Computing System.

Conflict of Interest statement: None declared.

Funding

This work was supported by a Developmental Award from the UCSF Breast Oncology Program and by grants from the NIH K24CA169004, CA120120 to E.Z.; the DoD Era of Hope W81XWH-12-1-0272 and the UCSF Breast Oncology Program Funding from the Atwater Family to A.G.; an NIH R01 GM071655 to S.B.; an NIH T32 Post-doctoral Training Grant (5T32CA108462-10) to A.Z. and a UCSF Graduate Research Mentorship Fellowship to R.C. Funding to pay the Open Access publication charges for this article was provided by grants from NCI (CA169004 and R21CA179442).

References

- Welter, D., MacArthur, J., Morales, J., Burdett, T., Hall, P., Junkins, H., Klemm, A., Flicek, P., Manolio, T., Hindorff, L. et al. (2014) The NHGRI GWAS Catalog, a curated resource of SNP-trait associations. *Nucl. Acids Res.*, **42**, D1001–D1006.
- Edwards, S.L., Beesley, J., French, J.D. and Dunning, A.M. (2013) Beyond GWASs: illuminating the dark road from association to function. *Am. J. Hum. Genet.*, **93**, 779–797.
- Freedman, M.L., Monteiro, A.N., Gayther, S.A., Coetzee, G.A., Risch, A., Plass, C., Casey, G., De Biasi, M., Carlson, C., Duggan, D. et al. (2011) Principles for the post-GWAS functional characterization of cancer risk loci. *Nat. Genet.*, **43**, 513–518.
- Li, Q., Seo, J.H., Stranger, B., McKenna, A., Pe'er, I., Laframboise, T., Brown, M., Tyekucheva, S. and Freedman, M.L. (2013) Integrative eQTL-based analyses reveal the biology of breast cancer risk loci. *Cell*, **152**, 633–641.
- Michailidou, K., Hall, P., Gonzalez-Neira, A., Ghoussaini, M., Dennis, J., Milne, R.L., Schmidt, M.K., Chang-Claude, J., Bojesen, S.E., Bolla, M.K. et al. (2013) Large-scale genotyping identifies 41 new loci associated with breast cancer risk. *Nat. Genet.*, **45**, 353–361, 361e351–352.
- Rhie, S.K., Coetzee, S.G., Noushmehr, H., Yan, C., Kim, J.M., Haiman, C.A. and Coetzee, G.A. (2013) Comprehensive functional annotation of seventy-one breast cancer risk Loci. *PLoS ONE*, **8**, e63925.
- Li, Q., Stram, A., Chen, C., Kar, S., Gayther, S., Pharoah, P., Hai-man, C., Stranger, B., Kraft, P. and Freedman, M.L. (2014) Ex-pression QTL-based analyses reveal candidate causal genes and loci across five tumor types. *Hum. Mol. Genet.*, **23**, 5294–5302.
- Cowper-Salari, R., Zhang, X., Wright, J.B., Bailey, S.D., Cole, M.D., Eeckhoutte, J., Moore, J.H. and Lupien, M. (2012) Breast cancer risk-associated SNPs modulate the affinity of chromatin for FOXA1 and alter gene expression. *Nat. Genet.*, **44**, 1191–1198.
- Lappalainen, T., Sammeth, M., Friedlander, M.R., Hoen, P.A., Monlong, J., Rivas, M.A., Gonzalez-Porta, M., Kurbatova, N., Griebel, T., Ferreira, P.G. et al. (2013) Transcriptome and genome sequencing uncovers functional variation in humans. *Nature*, **501**, 506–511.
- Pickrell, J.K., Marioni, J.C., Pai, A.A., Degner, J.F., Engelhardt, B.E., Nkadori, E., Veyrieras, J.B., Stephens, M., Gilad, Y. and Pritchard, J.K. (2010) Understanding mechanisms underlying human gene expression variation with RNA sequencing. *Nature*, **464**, 768–772.
- Kwan, T., Benovoy, D., Dias, C., Gurd, S., Provencher, C., Beaulieu, P., Hudson, T.J., Sladek, R. and Majewski, J. (2008) Genome-wide analysis of transcript isoform variation in humans. *Nat. Genet.*, **40**, 225–231.
- Pajares, M.J., Ezponda, T., Catena, R., Calvo, A., Pio, R. and Montuenga, L.M. (2007) Alternative splicing: an emerging topic in molecular and clinical oncology. *Lancet Oncol.*, **8**, 349–357.
- Shapiro, I.M., Cheng, A.W., Flytzanis, N.C., Balsamo, M., Condeelis, J.S., Oktay, M.H., Burge, C.B. and Gertler, F.B. (2011) An EMT-driven alternative splicing program occurs in human breast cancer and modulates cellular phenotype. *PLoS Genet.*, **7**, e1002218.
- Supek, F., Minana, B., Valcarcel, J., Gabaldon, T. and Lehner, B. (2014) Synonymous mutations frequently act as driver mutations in human cancers. *Cell*, **156**, 1324–1335.
- Cancer Genome Atlas, N. (2012) Comprehensive molecular portraits of human breast tumours. *Nature*, **490**, 61–70.
- Stegle, O., Parts, L., Durbin, R. and Winn, J. (2010) A Bayesian framework to account for complex non-genetic factors in gene expression levels greatly increases power in eQTL studies. *PLoS Comput. Biol.*, **6**, e1000770.
- Stegle, O., Parts, L., Piipari, M., Winn, J. and Durbin, R. (2012) Using probabilistic estimation of expression residuals (PEER) to obtain increased power and interpretability of gene expression analyses. *Nat. Protoc.*, **7**, 500–507.
- Anders, S., Reyes, A. and Huber, W. (2012) Detecting differential usage of exons from RNA-seq data. *Genome Res.*, **22**, 2008–2017.
- Steijger, T., Abril, J.F., Engstrom, P.G., Kokocinski, F., Consortium, R., Abril, J.F., Akerman, M., Alioto, T., Ambrosini, G., Antonarakis, S.E. et al. (2013) Assessment of transcript reconstruction methods for RNA-seq. *Nat. Methods*, **10**, 1177–1184.
- Pepke, S., Wold, B. and Mortazavi, A. (2009) Computation for ChIP-seq and RNA-seq studies. *Nat. Methods*, **6**, S22–S32.
- Harrow, J., Frankish, A., Gonzalez, J.M., Tapanari, E., Diekhans, M., Kokocinski, F., Aken, B.L., Barrell, D., Zaidis, A.,

- Searle, S. et al. (2012) GENCODE: the reference human genome annotation for The ENCODE Project. *Genome Res.*, **22**, 1760–1774.
22. Degner, J.F., Marioni, J.C., Pai, A.A., Pickrell, J.K., Nkadori, E., Gilad, Y. and Pritchard, J.K. (2009) Effect of read-mapping biases on detecting allele-specific expression from RNA-sequencing data. *Bioinformatics*, **25**, 3207–3212.
23. Pruim, R.J., Welch, R.P., Sanna, S., Teslovich, T.M., Chines, P.S., Gliedt, T.P., Boehnke, M., Abecasis, G.R. and Willer, C.J. (2010) LocusZoom: regional visualization of genome-wide association scan results. *Bioinformatics*, **26**, 2336–2337.
24. Kent, W.J., Sugnet, C.W., Furey, T.S., Roskin, K.M., Pringle, T.H., Zahler, A.M. and Haussler, D. (2002) The human genome browser at UCSC. *Genome Res.*, **12**, 996–1006.
25. Desmet, F.O., Hamroun, D., Lalande, M., Collod-Beroud, G., Claustres, M. and Beroud, C. (2009) Human Splicing Finder: an online bioinformatics tool to predict splicing signals. *Nucl. Acids Res.*, **37**, e67.
26. Dimas, A.S., Deutsch, S., Stranger, B.E., Montgomery, S.B., Borel, C., Attar-Cohen, H., Ingle, C., Beazley, C., Gutierrez Arcelus, M., Sekowska, M. et al. (2009) Common regulatory variation impacts gene expression in a cell type-dependent manner. *Science*, **325**, 1246–1250.
27. Consortium, G.-O. (2014). Dana-Farber Cancer Institute, Boston, MA, Vol. 2014.
28. Singh, G. and Cooper, T.A. (2006) Minigene reporter for identification and analysis of cis elements and trans factors affecting pre-mRNA splicing. *BioTechniques*, **41**, 177–181.
29. Coetzee, S.G., Rhie, S.K., Berman, B.P., Coetzee, G.A. and Noushmehr, H. (2012) FunciSNP: an R/bioconductor tool integrating functional non-coding data sets with genetic association studies to identify candidate regulatory SNPs. *Nucl. Acids Res.*, **40**, e139.
30. Consortium, E.P., Bernstein, B.E., Birney, E., Dunham, I., Green, E.D., Gunter, C. and Snyder, M. (2012) An integrated encyclopedia of DNA elements in the human genome. *Nature*, **489**, 57–74.
31. Schaub, M.A., Boyle, A.P., Kundaje, A., Batzoglou, S. and Snyder, M. (2012) Linking disease associations with regulatory information in the human genome. *Genome Res.*, **22**, 1748–1759.
32. Antoniou, A.C., Wang, X., Fredericksen, Z.S., McGuffog, L., Tarrell, R., Sinilnikova, O.M., Healey, S., Morrison, J., Kartsonaki, C., Lesnick, T. et al. (2010) A locus on 19p13 modifies risk of breast cancer in BRCA1 mutation carriers and is associated with hormone receptor-negative breast cancer in the general population. *Nat. Genet.*, **42**, 885–892.
33. Nica, A.C., Montgomery, S.B., Dimas, A.S., Stranger, B.E., Beazley, C., Barroso, I. and Dermitzakis, E.T. (2010) Candidate causal regulatory effects by integration of expression QTLs with complex trait genetic associations. *PLoS Genet.*, **6**, e1000895.
34. Giambartolomei, C., Vukcevic, D., Schadt, E.E., Franke, L., Hingorani, A.D., Wallace, C. and Plagnol, V. (2014) Bayesian test for colocalisation between pairs of genetic association studies using summary statistics. *PLoS Genet.*, **10**, e1004383.
35. Lev Maor, G., Yearim, A. and Ast, G. (2015) The alternative role of DNA methylation in splicing regulation. *Trends Genet.*, **31**, 274–280.
36. George, J., Lim, J.S., Jang, S.J., Cun, Y., Ozretic, L., Kong, G., Leenders, F., Lu, X., Fernandez-Cuesta, L., Bosco, G. et al. (2015) Comprehensive genomic profiles of small cell lung cancer. *Nature*, **524**, 47–53.
37. Consortium, G.T. (2013) The Genotype-Tissue Expression (GTEx) project. *Nat. Genet.*, **45**, 580–585.
38. Delaneau, O., Coulonges, C. and Zagury, J.F. (2008) Shape-IT: new rapid and accurate algorithm for haplotype inference. *BMC Bioinformatics*, **9**, 540.
39. Genomes Project, C., Abecasis, G.R., Auton, A., Brooks, L.D., DePristo, M.A., Durbin, R.M., Handsaker, R.E., Kang, H.M., Marth, G.T. and McVean, G.A. (2012) An integrated map of genetic variation from 1,092 human genomes. *Nature*, **491**, 56–65.
40. Howie, B.N., Donnelly, P. and Marchini, J. (2009) A flexible and accurate genotype imputation method for the next generation of genome-wide association studies. *PLoS Genet.*, **5**, e1000529.
41. Zheng, J., Li, Y., Abecasis, G.R. and Scheet, P. (2011) A comparison of approaches to account for uncertainty in analysis of imputed genotypes. *Genet Epidemiol.*, **35**, 102–110.
42. Qiu, X., Wu, H. and Hu, R. (2013) The impact of quantile and rank normalization procedures on the testing power of gene differential expression analysis. *BMC Bioinformatics*, **14**, 124.
43. Price, A.L., Patterson, N.J., Plenge, R.M., Weinblatt, M.E., Shadick, N.A. and Reich, D. (2006) Principal components analysis corrects for stratification in genome-wide association studies. *Nat. Genet.*, **38**, 904–909.
44. International HapMap, C. (2003) The International HapMap Project. *Nature*, **426**, 789–796.
45. Zaitlen, N., Pasaniuc, B., Gur, T., Ziv, E. and Halperin, E. (2010) Leveraging genetic variability across populations for the identification of causal variants. *Am. J. Hum. Genet.*, **86**, 23–33.
46. Han, B., Kang, H.M. and Eskin, E. (2009) Rapid and accurate multiple testing correction and power estimation for millions of correlated markers. *PLoS Genet.*, **5**, e1000456.